Attachment 9

Peach Bottom Atomic Power Station Units 2 and 3

NRC Docket Nos. 50-277 and 50-278

WCAP-17649, Rev 1, ASME Code Stress Report

Westinghouse Non-Proprietary Class 3

WCAP-17649-NP
Revision 1

February 2014

Peach Bottom Units 2 and 3 ASME Code Stress Report

(Enclosure B.3)

Westinghouse

WCAP-17649-NP
Revision 1

Peach Bottom Units 2 and 3 ASME Code Stress Report

Hari Srivastava*, PE
Principal Engineer, BWR Component & Installation Engineering

February 2014

Verifier: Yan Han*, PE
Principal Engineer, BWR Engineering

Approved: Gregory F. Vincent*, Manager
BWR Component & Installation Engineering

*Electronically approved records are authenticated in the electronic document management system.

Westinghouse Electric Company LLC
1000 Westinghouse Drive
Cranberry Township, PA 16066, USA

TABLE OF CONTENTS

LIST OF TABLES

LIST OF FIGURES

Trademark Note:

EXECUTIVE SUMMARY

Exelon is planning an extended power uprate (EPU) at Peach Bottom Atomic Power Station (PBAPS) Units 2 and 3 and plans to replace the existing stream dryers with replacement dryers at both units. Evaluation is performed to show compliance of the replacement dryers with the structural requirements of ASME B&PV Code, Section III, Division 1, Subsection NG. The evaluation shows that the dryers meet the stress and fatigue usage limits of the ASME Code for the EPU duty cycles covering normal operation (Service Level A), upset conditions (Service Level B), emergency conditions (Service Level C), and faulted conditions (Service Level D).

1 INTRODUCTION

In 2002, after increasing power to 117 percent of the original licensed thermal power, a steam dryer in a boiling water reactor (BWR) had a series of structural failures. Various industry experts evaluated and determined the root cause of the failures was fluctuating acoustic pressure loads on the steam dryer. The fluctuation resulted from resonances produced by steam flow in the main steam lines (MSLs) across safety valve and relief valve inlets. The failures in the steam dryer led to changes in Regulatory Guide 1.20 (Reference 1), requiring plants to evaluate their steam dryers before any planned increase in power level.

Exelon is planning extended power uprate (EPU) at Peach Bottom Atomic Power Station (PBAPS) Units 2 (PB2) and 3 (PB3) and plans to replace the existing stream dryers with replacement dryers at both units. The process used to qualify the replacement dryers for EPU operation involves scale model testing and multiple acoustic and structural analyses. High cycle fatigue calculations are performed using special purpose computer codes to calculate the acoustic loads together with finite element structural analyses using commercially available computer codes. The finite element models used for the acoustic analyses are also used in analyses to qualify the dryers for the ASME Code requirements.

The purpose of this report is to document analyses performed to show compliance of the replacement dryers with the structural requirements of ASME B&PV Code, Section III, Division 1, Subsection NG (Reference 2). Evaluations are performed for the PB2 replacement dryer with and without instrumentation mast assembly and for the PB3 replacement dryer. The evaluations show that the dryers meet the stress and fatigue usage limits of the ASME Code for the EPU duty cycles covering normal operation (Service Level A), upset conditions (Service Level B), emergency conditions (Service Level C), and faulted conditions (Service Level D).

In Revision 1, there have been many changes, as shown below. Therefore, no revision bars are used.

- Due to dryer design changes, the affected Tables in Section 2 and Section 4 are completely revised. Because of the design changes, Figure 2-1 and Figure 2-2 are revised.
- FIV stresses include the vane passing frequency (VPF) stress due to recirculation pump operation.
- Figure 4-5 to Figure 4-10 are revised to provide new stress distributions.
- Text in the report is revised accordingly to show these changes.

2 SUMMARY AND CONCLUSIONS

2.1 ANALYSIS

The dryers were analyzed with ANSYS® finite element code, Version 11.0 (Reference 3), running under the Microsoft Windows® 7 operating system, using 360° analysis models. The analysis model for the PB2 dryer with the instrumentation mast is shown in Figure 2-1and Figure 2-2. The analysis model for the PB2 dryer without the mast is similar except for removal of finite elements representing the mast assembly. The analysis model for the PB3 dryer is similar except for removal of finite elements representing the mast assembly and the hold-down rods, and changes in the lifting lug bracket model.

Analyses were performed for deadweight, differential pressures, seismic loads, Turbine Stop Valve (TSV) acoustic and flow reversal loads, and Main Steam Line Break (MSLB) differential pressure loads. Stresses for Flow Induced Vibration (FIV) loads, and recirculation pump Vane Passing Frequency (VPF) loads were based on the stress limits used to qualify the dryers for FIV/VPF loads (Reference 4). Stresses for MSLB acoustic loads were assumed to equal the maximum stresses calculated in separate analyses for the MSLB loads (Reference 5). Thermal loads were not considered because the dryer operates under isothermal conditions and the structural design does not have materials with different expansion coefficients.

The dryers were supported in vertical and circumferential directions at the support lugs for analyses, except analyses for MSLB differential pressure loads that produce a dryer lift-off. For lift-off analyses, the models were supported at the top of the dryer hold-down rods (PB2) or lifting rods (PB3) in the vertical direction and at the support lugs in the circumferential direction.

Surface loads were applied as pressure, gravity load was applied as equivalent static acceleration, and OBE and SSE loads were analyzed by response spectrum analyses.

2.2 DESIGN MARGINS

Component and weld stresses for the three dryer configurations (PB2 dryer with and without instrumentation mast, and PB3 dryer) for the specified load combinations, including the FIV/VPF and MSLB acoustic load stresses, are listed in Table 4-2 through Table 4-17. Maximum stresses extracted from these tables are compared with the ASME Code (Section III, Subsection NG) stress limits in Table 2-1 through Table 2-8 to calculate design margins applicable to all the dryer configurations.

Positive design margins are calculated for the specified load combinations with conservative assumptions, which include:

- Use of seismic response spectra for [ ]^{a,c} damping for OBE and SSE
- Except for two welds, assumption of all the components and welds to have FIV/VPF stresses equal to the ASME Code alternating endurance stress limits. For two of the welds, it was necessary to assume somewhat lower FIV/VPF stresses. However, the assumed FIV/VPF stresses were 40% larger than the weld stresses calculated in Reference 4.

- Assumption of the components and welds to have MSLB-acoustic stresses equal to the largest stress calculated in MSLB analyses.

- Addition of maximum stresses from different loads in a load combination while ignoring differences in locations of maximum stresses for the different types of loads.

- Use of maximum local mid-wall and surface stresses for comparison to membrane and membrane + bending stress limits without averaging or linearizing the stresses across sections.

- Classifying stresses from pressure loads at constrained plate boundaries as primary stresses (with lower stress limits) rather than secondary stresses (with higher stress limits) as classified by ASME Code Section III, Subsection NG, Table NG-3217-1.

Fatigue usage for ASME loads and concurrent FIV/VPF loads is insignificant [ ]^{a,c} compared to the ASME Code usage limit of 1.0. FIV/VPF loads independent of the ASME loads are shown to be well below the ASME Code endurance limit in Reference 4.

2.3 INTERFACE LOADS

Table 2-9 lists interface loads for use in evaluation of dryer support brackets and hold-down rods. The loads in the table are for a single support lug and a single hold-down bracket.

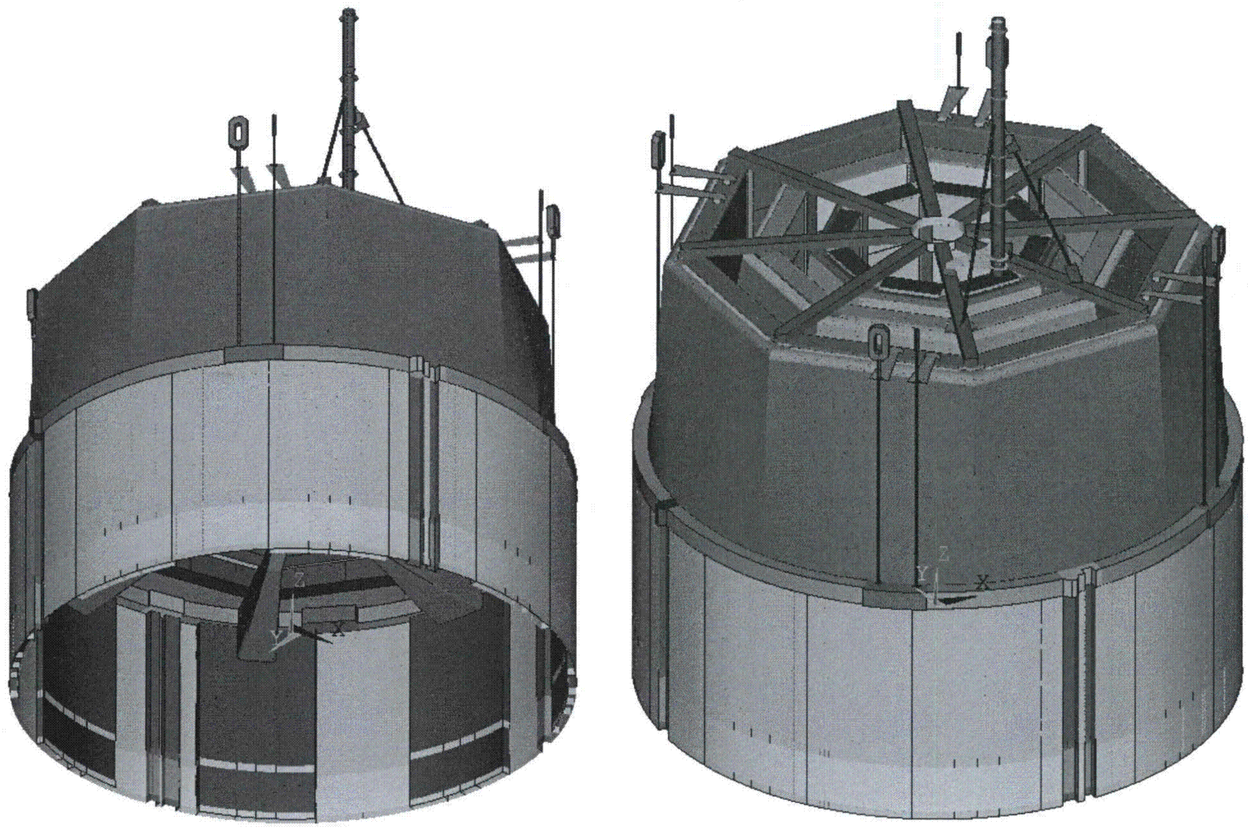

Figure 2-1 PB2 Dryer with Instrumentation Mast: Analysis Model - Outline

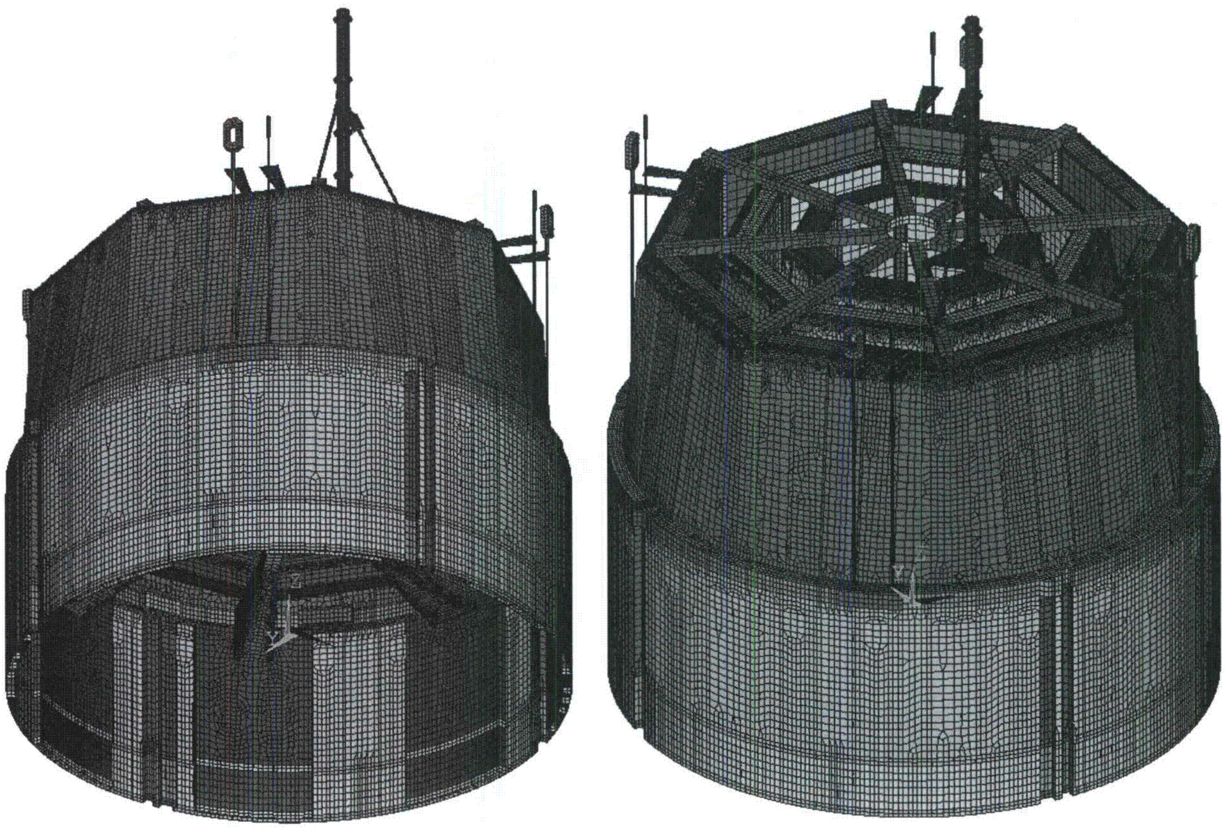

Figure 2-2 PB2 Dryer with Instrumentation Mast: Analysis Model - Finite Element Mesh

Table 2-1 Minimum Design Margins – Components (Service Level A)

a,c

Table 2–1 Minimum Design Margins – Components (Service Level A) (cont.)

a,c

Table 2-2 Minimum Design Margins – Welds (Service Level A)

a,c

Table 2–2 Minimum Design Margins – Welds (Service Level A) (cont.)

a,c

Table 2–2 Minimum Design Margins – Welds (Service Level A) (cont.)

a,c

Table 2–2 Minimum Design Margins – Welds (Service Level A) (cont.)

a,c

Table 2-3 Minimum Design Margins – Components (Service Level B)

a,c

Table 2-3 Minimum Design Margins – Components (Service Level B) (cont.)

a,c

Table 2-4 Minimum Design Margins – Welds (Service Level B)

a,c

Table 2–4 Minimum Design Margins – Welds (Service Level B) (cont.)

a,c

Table 2–4 Minimum Design Margins – Welds (Service Level B) (cont.)

a,c

Table 2–4 Minimum Design Margins – Welds (Service Level B) (cont.)

a,c

Table 2-5 Minimum Design Margins – Components (Service Level C)

a,c

Table 2–5 Minimum Design Margins – Components (Service Level C) (cont.)

a,c

Table 2-6 Minimum Design Margins – Welds (Service Level C)

a,c

Table 2–6 Minimum Design Margins – Welds (Service Level C) (cont.)

a,c

Table 2–6 Minimum Design Margins – Welds (Service Level C) (cont.)

a,c

Table 2–6 Minimum Design Margins – Welds (Service Level C) (cont.)

a,c

Table 2-7 Minimum Design Margins – Components (Service Level D)

a,c

Table 2–7 Minimum Design Margins – Components (Service Level D) (cont.)

a,c

Table 2-8 Minimum Design Margins – Welds (Service Level D)

a,c

Table 2–8 Minimum Design Margins – Welds (Service Level D) (cont.)

a,c

Table 2-8 Minimum Design Margins – Welds (Service Level D) (cont.)

a,c

Table 2-8 Minimum Design Margins – Welds (Service Level D) (cont.)

a.c

Table 2-9 Reaction Loads

a,c

3 ANALYSIS INPUT

3.1 LOADS

Specified loads are Deadweight, Differential Pressures (DP) from a pressure drop across the dryer vane banks, and TSV and MSLB loads on the outer hoods. Thermal loads are not considered because the dryer operates in isothermal environment and the structural design does not involve materials with different thermal expansion coefficients.

3.1.1 Gravity

The dryer weight is included in the analysis models by specifying component dimensions and material densities.

3.1.2 Pressure Loads

Normal Operation, Upset Condition, and Emergency Condition pressure differences across the dryer (Reference 6) are listed in Table 3-1 as DP_N, DP_U, and DP_E, respectively. Pressures following MSLB are listed as $MSLB_{DP1}$ and $MSLB_{DP2}$.

Reactor Thermal Cycles Diagram (Reference 7) identifies [ ]^{a,c} start-up cycles and [ ]^{a,c} operational scrams. Because potential pressure reductions during the scram events are not defined, the start-up and scram cycles were added [ ]^{a,c} and enveloped by using [ ]^{a,c} load cycles for fatigue usage calculations.

TSV loads (Reference 8) on the outer hoods are listed in Table 3-2. Acoustic load TSV_A is shown as pressure distribution relative to the center line of the affected steam line. The reverse flow impingement load following the valve closure is listed as TSV_F. TSV_F, not to be combined with TSV_A, acts on the outer hood area corresponding to projection of the steam nozzle on the outer hood.

For fatigue usage calculations, [ ]^{a,c} TSV stress cycles are specified (Reference 9).

FIV/VPF loads and MSLB acoustic loads are described and analyzed separately (Reference 4 and Reference 5). Stresses from these analyses were enveloped and combined with stresses calculated in present analyses as described in Section 4.

Table 3-1 Dryer Pressure Loads (Reference 6)	
DP_N, Normal Operation pressure, psid	[ ]^{a,c}
DP_U, Upset Condition pressure, psid	[ ]^{a,c}
DP_E, Emergency Condition pressure, psid	[ ]^{a,c}
$MSLB_{DP1}$, MSLB outside containment, rated power and core flow condition, psid	[ ]^{a,c}
$MSLB_{DP2}$, MSLB outside containment, low power / high core flow condition, psid[(1)]	[ ]^{a,c}
Note: (1) Limit load analysis was performed to justify higher pressure (Reference 12)	

Table 3-2 TSV Loads on the Outer Hood (Reference 8)

a,c

3.1.3 Seismic Loads

Specific N-S and E-W response spectra for [ ]^{a,c} damping (Reference 10) are shown in Figure 3-1. These spectra were enveloped and used as horizontal OBE and SSE loads. Two-thirds of the enveloped spectra in the figure were used for Vertical seismic loads (Reference 9).

For fatigue usage calculations, [ ]^{a,c} OBE stress cycles are used (Reference 9).

3.2 LOAD COMBINATIONS

Table 3-3 lists the specific load combinations (Reference 9). When combining seismic loads:

1. Stresses from N-S and vertical excitations are to be combined using absolute summation.

2. Stresses from E-W and vertical excitations are to be combined using absolute summation.

3. The larger of the N-S-vertical seismic stresses and E-W-vertical seismic stresses are to be used with stresses from other loads to obtain stresses for specific load combinations.

Table 3-3 Load Combinations (Reference 9)

Load Case	Service Condition	Acceptance Criteria (Service Level)	Operating Condition	Load Combination
A	Normal	A	Normal Operation	$DW + DP_N + FIV$
B-1	Upset	B	Turbine Stop Valve Closure (Acoustic Load)	$DW + DP_N + ((TSV_A)^2 + (FIV)^2)^{1/2}$
B-2	Upset	B	Turbine Stop Valve Closure (Flow Reversal Load)	$DW + DP_N + TSV_F$
B-3	Upset	B	Normal Operation plus OBE plus FIV	$DW + DP_N + ((OBE)^2 + (FIV)^2)^{1/2}$
B-6	Upset	B	DW, Differential Pressure (Upset) plus FIV	$DW + DP_U + FIV$
C-1	Emergency	C	DW, Differential Pressure (Emergency) plus FIV	$DW + DP_E + FIV$
D-3	Faulted	D	Normal plus FIV plus SSE plus DBA	$DW + DP_N + ((MSLB_{A1})^2 + (SSE)^2 + (FIV)^2)^{1/2}$
D-4	Faulted	D	Normal plus FIV plus SSE plus DBA	$DW + DP_N + ((MSLB_{A2})^2 + (SSE)^2 + (FIV)^2)^{1/2}$
D-5	Faulted	D	Normal plus SSE plus DBA	$DW + MSLB_{DP1} + SSE$
D-6	Faulted	D	Normal plus DBA	$DW + MSLB_{DP2}$

Legend:

DW Deadweight (+ weight of entrapped water for dynamic analysis)

DP_N Differential pressure - normal operation

DP_U Differential pressure - upset condition

DP_E Differential pressure - emergency condition

FIV Flow induced vibration loads (plus Vane Passing Frequency (VPF) loads)

TSV_A Acoustic load caused by closure of Turbine Stop Valve.

TSV_F Flow impingement load caused by closure of Turbine Stop Valve.

OBE OBE inertia load (anchor displacement loads are negligible)

SSE SSE inertia load (anchor displacement loads are negligible)

DBA Design Basis Accident

- $MSLB_{A1}$ Acoustic rarefaction wave load due to MSLB outside the containment, rated power and core flow condition
- $MSLB_{A2}$ Acoustic rarefaction wave load due to MSLB outside the containment, low power / high core flow condition
- $MSLB_{DP1}$ Differential Pressure load due to MSLB outside the containment, rated power and core flow condition
- $MSLB_{DP2}$ Differential Pressure load due to MSLB outside the containment, low power / high core flow condition

3.3 ACCEPTANCE CRITERIA

The steam dryer is not an ASME B&PV Code component. However, it is evaluated as an Internal Structure according to the design rules of ASME B&PV Code, Section III, Division 1, Subsection NG (Reference 2). The applicable design rules are summarized in Table 3-4. The TSV pressure loads (Reference 8) in the analysis far exceed the normal operation ([ ][a,c]) and upset condition ([ ][a,c]) pressure loads (Reference 6) generally used for defining design pressure. Therefore, when applying the Service Level B stress limits to the TSV pressure loads, the stress limits were based on 110% of S_m values, according to Paragraph NG-3223 of the Code.

Table 3-4 Stress Limits (Reference 2)

Service level	Stress category	Stress limit
Service levels A & B[(1)]	P_m	S_m
	$P_m + P_b$	1.5 S_m
	Shear stress	0.6 S_m
	Bearing stress	S_y, (1.5 S_y away from free edge)
	Σ fatigue usage	1.0
Service level C	P_m	1.5 S_m
	$P_m + P_b$	2.25 S_m
	Shear stress	0.9 S_m
	Bearing stress	1.5 S_y, (2.25 S_y away from free edge)
Service level D	P_m	Min(2.4 S_m, 0.7 S_u)
	$P_m + P_b$	Min(3.6 S_m, 1.05 S_u)
	Shear stress	1.2 S_m
	Bearing stress	2.0 S_y, (3.0 S_y away from free edge)

Legend:

- P_m Primary membrane stress intensity
- P_b Primary bending stress intensity
- S_m Stress intensity limit
- S_y Yield strength
- S_u Ultimate strength

Note (1) TSV pressure exceeds the specified normal operation ([ ][a,c]) and upset condition pressure ([ ][a,c]) considered as design pressure and was evaluated using stress intensity value of 110% S_m according to Paragraph NG-3223 of Reference 2.

3.4 MATERIAL PROPERTIES

Dryer structural components are made from SA-240 type 316L. Table 3-5 lists the material properties (Reference 11) used in the analysis.

Table 3-5 Material Properties (Reference 11)

Material property	70°F	551°F
S_m, Stress intensity limit, psi	16,700	14,400
S_y, Yield strength, psi	25,000	16,000
S_u, Ultimate strength, psi	70,000	61,700
E, Young's modulus, psi	28.3×10^6	25.42×10^6

a,c

Figure 3-1 Seismic Response Spectra

4 ANALYSIS AND RESULTS

4.1 ANALYSIS MATRIX

Finite element analyses were performed for the PB2 dryer, PB2 dryer with instrumentation mast, and the PB3 dryer. In each case, analyses were performed for deadweight (DW), differential pressures (DP_N, DP_U, DP_E, $MSLB_{DP1}$, $MSLB_{DP2}$), seismic loads (OBE, SSE), and TSV loads (TSV_A, TSV_F). The hydrodynamic mass of the skirt was included in analyses for dynamic loads. FIV/VPF and $MSLB_A$ ($MSLB_{A1}$ and $MSLB_{A2}$) loads are developed and analyzed separately (Reference 4 and Reference 5). Maximum stresses from these analyses were enveloped and combined with the results of present analyses.

Table 4-1 lists the load cases included in the present analyses.

a,c

Table 4-1 Analysis Matrix

4.2 ANALYSIS

4.2.1 Analysis Model

Analysis models include the dryer skirt and drain channels, gussets, center plate and center ring, drain troughs and trough stiffeners, vane bank end plates, top plates, side plates, bank-to-bank attachment plates, and perforated plates, hoods, and upper girder assembly, all modeled with shell elements, dryer support ring modeled with solid elements, and lifting rods, hold-down rods, and vane bank tie rods modeled with beam elements. Dryer vanes are modeled as solid elements with weight equal to the vane bank weight. The hydrodynamic mass is modeled by adjusting density of the under-water elements of the skirt. The analysis model for the PB2 dryer with instrumentation mast is shown in Figure 2-1 and Figure 2-2. Analysis models for the PB2 dryer without instrumentation mast and the PB3 dryer are similar, except for the absence of the mast assembly in both of these models, and the absence of hold-down rods and different lifting lug bracket design in the PB3 dryer model.

4.2.2 Boundary Conditions

Dryers were supported in vertical and circumferential directions at the dryer support lugs for all the analyses, except for the analyses for $MSLB_{DP1}$ and $MSLB_{DP2}$ loads, which produce a dryer lift off. For lift-off analyses, the dryers were supported at the top of the lifting rods or hold-down rods in the vertical direction and at the support lugs in the circumferential direction.

Boundary conditions are shown in Figure 4-1 and Figure 4-2.

4.2.3 Load Application

For static analyses, pressure was applied as a surface load and gravity load was applied as 1g equivalent static acceleration. OBE and SSE loads were analyzed in response spectrum analyses.

TSV loads are specified in Table 3-2 as a pressure distribution and impingement load on the hood relative to one of the four Main Steam Line (MSL) nozzles. For the analysis, the specified acoustic load pressure distribution was assumed to apply at all the four MSLs in order to envelop the effects of acoustic wave propagation through the steam circuit. For consistency, the flow impingement load was also assumed to apply to all the four MSLs.

Figure 4-3 and Figure 4-4 show the pressure load application.

4.2.4 Load Combination Approach

Analyses were performed for the 14 load cases listed in Table 4-1. Relatively large middle hood displacements were calculated for Load Cases 7 ([ ]^{a,c}) and 8 ([ ]^{a,c}) because of the large pressures acting on the thin hood plates. With the small bending stiffness compared to the in-plane stiffness of the hoods, large transverse displacements would be accompanied by in-plane tensile forces resisting the deformations. The stress-stiffening option of ANSYS software was used to account for this coupling between the in-plane and out-of-plane deformations of the hoods.

Results of Load Cases 2, 3, 4, 5, 6, 7, and 8 were used directly for Load Combinations A, B-1, B-2, B-6, C-1, D-5, and D-6, respectively, in Table 3-3. OBE and SSE results for use in load combinations B-3, D-3, D-4, and D-5 were obtained from the response spectrum analyses of Load Cases 9 through 14 using the following approach:

1. Modal responses for each of the Load Cases 9 through 14 were combined using the Square Root of the Sum of the Squares (SRSS) approach to obtain OBE_X, OBE_Y, OBE_Z, SSE_X, SSE_Y, and SSE_Z responses, where Z is the vertical direction.

2. Vertical and horizontal direction responses were combined using absolute addition to obtain:

[

]]a,c

3. Maximum stress intensities for each dryer component were extracted for OBE_{XZ}, OBE_{YZ}, SSE_{XZ}, and SSE_{YZ}. These values were compared, ignoring differences in their locations in the components, to obtain maximum component seismic stress intensities as:

[

]a,c

OBE stresses were combined with the maximum normal operation stresses (Load Case 2) and maximum FIV/VPF stresses to obtain stresses for Load Combination B-3 using the following relationship:

[ ]a,c

SSE stresses were combined with the maximum normal operation stresses (Load Case 2), maximum FIV/VPF stresses, and maximum $MSLB_A$ ($MSLB_{A1}$ and $MSLB_{A2}$) stresses to obtain enveloping stresses for Load Combinations D-3 and D-4 using the following relationship:

[ ]a,c

SSE stresses were combined with the maximum ($DW+MSLB_{DP1}$) stresses (Load Case 7) to obtain stresses for Load Combination D-5 using the following relationship:

[ ]a,c

It was not possible to SRSS the TSV_A and FIV/VPF stresses because TSV_A + DW + DP_N loads were analyzed together (Load Case 3). Therefore, FIV/VPF stresses were added absolutely to the results for Load Case 3 to obtain stresses for Load Combination B-1.

The above approach of combining maximum stresses from different load cases to obtain maximum stresses for a Load Combination conservatively ignores the differences in the locations of maximum stresses for the different load cases.

4.2.5 Component Stresses

Maximum stresses in the dryer components are highly localized at nodes at intersections of weld lines between multiple components. Usually, such local stresses are used for fatigue calculations, and stresses away from these nodes are averaged and linearized across component sections and used for stress limit comparisons. However, the complex geometry of the dryer, large stress gradients, and differences in locations of maximum stresses for different loads make it difficult to select sections for stress averaging. Therefore, the following conservative approach was used for design margin calculations.

1. ANSYS post-processor was used to extract maximum mid-wall and surface stresses for each component modeled with shell elements including the elements at the weld lines, and the

maximum stresses anywhere in the components modeled with solid elements including the elements at the weld lines.

2. Maximum mid-wall and surface stresses from different loads in load combinations were combined as described in Section 4.2.4, conservatively ignoring differences in their locations in the components.

3. FIV/VPF loads are developed and analyzed separately (Reference 4). Component stresses in these analyses are limited to the ASME Code limit ([ ]^{a,c} psi) adjusted for elastic modulus ratio [ ]^{a,c}, and divided by a safety factor of S ≥ 1^{a,c}, or [ ]^{a,c}. For the ASME Code analysis, these stresses were enveloped by conservatively assuming maximum FIV/VPF stress in each component to equal the stress limit of [ ]^{a,c} psi, corresponding to a safety factor of 1. That is, all the components in the dryer were assumed to have a maximum surface stress of [ ]^{a,c} psi.

4. Maximum $MSLB_A$ ($MSLB_{A1}$ and $MSLB_{A2}$) surface stress of [ ]^{a,c} psi has been calculated in $MSLB_A$ analyses of the three dryer configurations (Reference 5). The high $MSLB_A$ stresses are in the outer hood region. Much lower stresses occur in other regions of the dryer. However, these maximum stresses were conservatively assumed to apply as surface stresses for all the components in the dryers.

5. As pressure loading produces primarily bending stresses with small membrane stresses, mid-wall stresses were enveloped by assuming a mid-wall FIV/VPF stress of [ ]^{a,c} psi and a mid-wall $MSLB_A$ stress of [ ]^{a,c} psi for all the components in the dryers.

6. The enveloping FIV/VPF and $MSLB_A$ stresses described in Steps (3-5) were added to the maximum component stresses calculated in Step (2) as described in Section 4.2.4. The resulting mid-wall stresses were compared with membrane stress limits without any averaging, and surface stresses were compared with membrane + bending stress limits without any linearizing.

7. In a few cases, maximum surface stresses described in Step (6) exceeded the membrane plus bending stress limit. Stress distributions in these cases were investigated in greater detail as described in Section 4.2.5.4.

The approach described above was used for each of the three dryer analysis models. Analysis results for the three dryers are discussed in terms of the following components:

Troughs	Gussets (thin section)	Gussets (thick section)
Gussets center plate	Gussets center ring	Trough stiffeners
VB (Vane Bank) end plates	VB top plates	VB top steps
VB top side plates	Inner hoods	Middle hoods
Outer hoods	VB to VB vertical plates	VB to VB top plates
Center cover plate	Upper girders	Upper girders center ring
Support ring	Drain channel	Skirt
Skirt slots	Skirt belts	Drain channel belts
Horizontal rails	Slot belts	

4.2.5.1 PB2 Dryer with Instrumentation Mast

Maximum mid-wall and surface stresses for components of the PB2 dryer with instrumentation mast are listed in Table 4-2 for load cases 2 through 8 and for OBE and SSE with directional earthquake stresses combined and maximized as described in Section 4.2.4.

Maximum stresses listed in Table 4-2 are combined following the approach described above to obtain mid-wall and surface stresses for various load combinations. These stresses are listed in Table 4-3. In listing the stresses, maximums of the stresses for Load Combinations D-3 and D-4 are reported in a common column.

4.2.5.2 PB2 Dryer without Instrumentation Mast

Maximum mid-wall and surface stresses for components of the PB2 dryer without instrumentation mast are listed in Table 4-4 for load cases 2 through 8 and for OBE and SSE with directional earthquake stresses combined and maximized as described in Section 4.2.4.

Maximum stresses listed in Table 4-4 are combined following the approach described above to obtain mid-wall and surface stresses for various load combinations. These stresses are listed in Table 4-5. In listing the stresses, maximums of the stresses for Load Combinations D-3 and D-4 are reported in a common column.

4.2.5.3 PB3 Dryer

Maximum mid-wall and surface stresses for the PB3 dryer components are listed in Table 4-6 for load cases 2 through 8 and for OBE and SSE with directional earthquake stresses combined and maximized as described in Section 4.2.4.

Maximum stresses listed in Table 4-6 are combined following the approach described above to obtain mid-wall and surface stresses for various load combinations. These stresses are listed in Table 4-7. In listing the stresses, maximums of the stresses for Load Combinations D-3 and D-4 are reported in a common column.

4.2.5.4 All Dryers

Stresses listed in Table 4-3, Table 4-5, and Table 4-7 for the three dryer configurations were compared to extract maximum stresses for the 10 load combinations (reported with combined maximum values for Load Combinations D-3 and D-4), which were further compared to obtain maximum stresses for the four ASME Code Service Levels. These stresses are listed in Table 4-8 together with the membrane and membrane + bending stress limits for the four Service Levels.

The conservatively calculated maximum stresses are within the ASME Code limit with two exceptions:

1. Service Levels A and B

   Service Level A and B surface stresses for Middle Hood, Outer Hood, Vane Bank (VB) Top Steps, and VB Top Side plates are close to or exceed the ASME Code primary stress limits. The stresses listed in the stress tables generally occur at multi-plate junctions as a result of deformation constraints. These stresses are highly localized and decrease to acceptable values within a small distance from the constraint location. This is illustrated in the surface stress plots for the PB2 dryer with instrumentation mast for $DW+DP_N$ loads in Figure 4-5 (Middle hood), Figure 4-6 (Outer hood), Figure 4-7 (VB top steps), and Figure 4-8 (VB top side plates). As shown in the top plot in each figure, maximum stresses are localized at intersections of multiple plates rather than in the main plate regions of the plates or along the welds. Removing elements at the constraint node decreases the stresses by [ ]^{a,c} or more as shown in the bottom plot of each figure. (The maximum stresses in figures are smaller than the corresponding stresses in the stress tables. This is because it was necessary to include multiple plates in the figures to show that the maximum stresses occur at their junctions. The angles between the plates result in smaller nodal stress averages compared to the stress tables, which were based on stress distributions in individual plates).

   Thus, the listed maximum stresses are local stresses that produce fatigue usage but do not significantly contribute to membrane and bending stresses. Therefore, stresses for code comparison can be obtained by removing elements at the maximum stress locations while maintaining the conservatism. Accordingly, elements attached to the node corresponding to the maximum stress locations were removed and maximum stresses were extracted from the rest of the stress distributions. This was done only for components and Load Combinations producing local stresses in excess of the stress limits. The resulting stresses are listed in Table 4-9 and reported for design margin results (Table 2-1and Table 2-3). Note that the approach of removing local peak stresses does not affect the maximum stress for the TSV acoustic pressure load because the maximum stresses occur away from welds as shown in Figure 4-9. Otherwise, the stresses listed in the table after removing the maximum stress elements are still local peaks stresses rather than section-averaged stresses and provide conservative estimates of design margins.

2. Service Level D

   The Middle hood surface stress of [ ]^{a,c} psi exceeds the ASME Code Service Level D Pm+Pb limit of [ ]^{a,c} psi for elastic analysis. Figure 4-10 shows that the overstress condition occurs in the middle hood for the $MSLB_{DP2}$ pressure load.

With the stress limit for elastic analysis exceeded, collapse analyses were performed (Reference 12) for the middle hood assuming elastic-perfectly plastic behavior and a yield stress of [ ]^{a,c} psi following Appendix F of the ASME Code (Reference 13). A quarter-model of the hood was analyzed with symmetry boundary conditions applied at the symmetry (vertical) boundaries. Analyses were performed with the upper and lower edges of the hood 1) fixed against displacements, and 2) fixed against displacements and rotations. Increasing pressure load was applied until collapse was indicated by rapid increase in displacements and lack of convergence.

Collapse pressures of [ ]^{a,c} psi and [ ]^{a,c} psi were calculated for the case with upper and lower edges of the hood fixed only against displacements, and the case with the edges fixed against displacements and rotations, respectively. Using the ASME design limit of 0.9 × collapse pressure (Reference 13) with the lower value of collapse pressure gives a pressure limit of [ ]^{a,c} psi, which provides adequate design margin for the $MSLB_{DP2}$ pressure of [ ]^{a,c} psi.

Table 4-2 PB2 Dryer with Mast, Load Cases 2-14, Maximum Component Stresses

a,c

Table 4–2 PB2 Dryer with Mast, Load Cases 2-14, Maximum Component Stresses (cont.)

a,c

Table 4–2 PB2 Dryer with Mast, Load Cases 2-14, Maximum Component Stresses (cont.)

a,c

Table 4-3 PB2 Dryer with Mast, Load Combinations, Maximum Component Stresses

a,c

Table 4–3 PB2 Dryer with Mast, Load Combinations, Maximum Component Stresses (cont.)

a,c

Table 4–3 PB2 Dryer with Mast, Load Combinations, Maximum Component Stresses (cont.)

a,c

Table 4-4 PB2 Dryer without Mast, Load Cases 2-14, Maximum Component Stresses

a,c

Table 4-4 PB2 Dryer without Mast, Load Cases 2-14, Maximum Component Stresses (cont.)

a,c

Table 4-4 PB2 Dryer without Mast, Load Cases 2-14, Maximum Component Stresses (cont.)

a,c

Table 4-5 PB2 Dryer without Mast, Load Combinations, Maximum Component Stresses

a,c

Table 4-5 PB2 Dryer without Mast, Load Combinations, Maximum Component Stresses (cont.)

a,c

Table 4–5 PB2 Dryer without Mast, Load Combinations, Maximum Component Stresses (cont.)

a,c

Table 4-6 PB3 Dryer, Load Cases 2-14, Maximum Component Stresses

a,c

Table 4–6 PB3 Dryer, Load Cases 2-14, Maximum Component Stresses (cont.)

a,c

Table 4-6 PB3 Dryer, Load Cases 2-14, Maximum Component Stresses (cont.)

a,c

Table 4-7 PB3 Dryer, Load Combinations, Maximum Component Stresses

a,c

Table 4–7 PB3 Dryer, Load Combinations, Maximum Component Stresses (cont.)

a,c

Table 4-7 PB3 Dryer, Load Combinations, Maximum Component Stresses (cont.)

a,c

Table 4-8 All Dryers, Service Levels, Maximum Component Stresses

a,c

Table 4-9 Maximum Component Stresses After Removing Elements at Maximum Stress Locations

a,c

4.2.6 Weld Stresses

Weld stresses were calculated using the same approach as used for component stress calculations in that maximum weld stresses for individual loads were extracted and combined according to specific load combinations without taking credit for differences in locations of maximum stresses, and local maximum stresses were used for stress comparison without averaging over potential failure lengths.

Different FIV/VPF stresses were used in weld calculations compared to the component stresses. The ASME alternating stress limit of [ ][a,c] psi used as FIV/VPF stress in the dryer components was divided by the minimum Stress Concentration factor **f** = 1.4 used in FIV/VPF analyses (Reference 4) to obtain the corresponding weld stress limit of [ ][a,c] psi. The maximum stress of [ ][a,c] psi calculated in MSLB$_A$ (MSLB$_{A1}$ and MSLB$_{A2}$) analyses (Reference 5) would envelop the weld as well as component stresses. With these considerations, FIV/VPF and MSLB$_A$ surface stresses at all welds were assumed to be [ ][a,c] psi and [ ][a,c] psi, respectively, and FIV/VPF and MSLB$_A$ mid-wall stresses at all welds were assumed to be [ ][a,c] psi and [ ][a,c] psi, respectively.

Weld stresses for the individual load cases for the PB2 dryer with mast, the PB2 dryer without mast, and the PB3 dryer are shown in Table 4-10, Table 4-12, and Table 4-14, respectively. Corresponding stresses for the various load combinations are shown in Table 4-11, Table 4-13, and Table 4-15, respectively. The maximum weld stresses for the four Service Levels, which are obtained by comparing the three dryer stresses for each Service Level's load combination, are listed in Table 4-16 together with the ASME Code stress limits for weld quality factors of **n** = 0.75 and 0.9. All the welds are full penetration welds to be examined with root and final PT (**n** = 0.75), except for the Middle Hood vertical welds, which are to be examined with progressive PT (**n** = 0.90).

The conservatively calculated local maximum stresses are within the stress limits for most of the welds. Exceptions in which the stresses exceed the stress limits are identified in Table 4-16. As discussed in

Section 4.2.5.4, the reported stresses are local stresses from deformation constraints at multiple-plate junctions. Although used in calculating fatigue usage with appropriate weld strength reduction factor *f* ([ ]^{a,c} for full penetration welds), they do not contribute significantly to membrane and bending stresses. Therefore, elements at maximum stress locations were removed and maximum stresses were extracted from the rest of the stress distributions. This was done only for welds and Load Combinations producing local stresses in excess of the stress limits. The resulting stresses are listed in Table 4-17. With a few exceptions, the highest stresses for different Service Levels in Table 4-17 are directly used for design margin results (Table 2-2, Table 2-4, Table 2-6 and Table 2-8). For long welds, maximum stresses occur at mid-length locations in addition to the ends. The high stresses at mid-length locations are not affected by removing a few high-stress elements and exceed the stress limits for the welds listed in the following table. Approaches used to resolve them are discussed in the following paragraph.

Weld / load combination	Maximum surface stress, psi	
	(All elements)	(After removing elements at the peak maximum stress nodes)
B1: $DW+DP_N+TSV_A+FIV$		
vb-top step to outer hoods	[ ]^{a,c}	[ ]^{a,c}
outer hood to outer hood	[ ]^{a,c}	[ ]^{a,c}
B3: DW+DPN+OBE+FIV		
vb-vb vert plate to middle hood	[ ]^{a,c}	[ ]^{a,c}

Maximum stresses for the vane bank top step to outer hood welds ([ ]^{a,c} psi) and the outer hood to outer hood welds ([ ]^{a,c} psi) exceed the ASME stress limit of [ ]^{a,c} psi. However, the stresses result from the TSV_A loads (Load Combination B1) assumed to originate from two adjacent Main Steam Lines, producing a [ ]^{a,c} psi to [ ]^{a,c} psi pressure load. This exceeds the normal operation and upset condition pressures of [ ]^{a,c} psi and [ ]^{a,c} psi, respectively. Therefore, the TSV_A pressure can be considered much larger than the design pressure, for which the Code specifies 10% higher Service Level B stress limits. These higher limits are used to calculate design margins for these two weld/load combination stresses.

In addition, it was necessary to assume FIV/VPF weld stresses of [ ]^{a,c} psi (outer hood to outer hood) and [ ]^{a,c} psi (vb-vb vert plate to middle hood welds) instead of the [ ]^{a,c} psi FIV/VPF stress used for the remaining welds and load combinations in order to meet the stress limits. The following table shows the weld stress calculated with these assumptions, and used for design margin calculations (Table 2-4). Note that the FIV/VPF stresses are not directly additive for two of the welds, but are added using SRSS because the controlling load combinations involve OBE.

The corresponding FIV/VPF stresses calculated for these welds in Reference 4 are [ ]^{a,c} psi, [ ]^{a,c} psi, and [ ]^{a,c} psi instead of [ ]^{a,c} psi, [ ]^{a,c} psi, and [ ]^{a,c} psi assumed in the present evaluation for the outer hood to outer hood welds, vb-vb vertical plate to middle hood welds, and vb top step to outer hood welds, respectively.

Weld / load combination	Assumed FIV stress, psi	Maximum weld surface stress, psi
vb-top step to outer hoods	[ ]a,c	[ ]a,c
outer hood to outer hood	[ ]a,c	[ ]a,c
vb-vb vert plate to middle hood	[ ]a,c	[ ]a,c

4.2.7 Interface Loads

Table 2-9 lists the maximum reaction loads imposed by the dryer on the dryer support lugs and the lifting-rod hold-down brackets. The loads were calculated considering static equilibrium of pressure loads, seismic loads based on ZPA, and dryer weight. It was considered acceptable to use ZPA because the frequency of the structural components in the dryer is ~[ ]a.c Hz, which is close to the response spectra ZPA (Figure 3-1). The loads are the maximum loads on a support bracket, a hold-down rod (PB2), or a lifting rod (PB3).

Table 4-10 PB2 Dryer with Mast, Load Cases 2-14, Maximum Weld Stresses

a,c

Table 4–10 PB2 Dryer with Mast, Load Cases 2-14, Maximum Weld Stresses (cont.)

a,c

Table 4–10 PB2 Dryer with Mast, Load Cases 2-14, Maximum Weld Stresses (cont.)

a,c

Table 4–10 PB2 Dryer with Mast, Load Cases 2-14, Maximum Weld Stresses (cont.)

a,c

Table 4–10 PB2 Dryer with Mast, Load Cases 2-14, Maximum Weld Stresses (cont.)

a,c

Table 4–10 PB2 Dryer with Mast, Load Cases 2-14, Maximum Weld Stresses (cont.)

a,c

Table 4-11 PB2 Dryer with Mast, Load Combinations, Maximum Weld Stresses

a,c

Table 4–11 PB2 Dryer with Mast, Load Combinations, Maximum Weld Stresses (cont.)

a,c

Table 4–11 PB2 Dryer with Mast, Load Combinations, Maximum Weld Stresses (cont.)

a,c

Table 4–11 PB2 Dryer with Mast, Load Combinations, Maximum Weld Stresses (cont.)

a,c

Table 4–11 PB2 Dryer with Mast, Load Combinations, Maximum Weld Stresses (cont.)

a,c

Table 4–11 PB2 Dryer with Mast, Load Combinations, Maximum Weld Stresses (cont.)

a,c

Table 4-12 PB2 Dryer without Mast, Load Cases 2-14, Maximum Weld Stresses

a,c

Table 4–12 PB2 Dryer without Mast, Load Cases 2-14, Maximum Weld Stresses (cont.)

a,c

Table 4–12 PB2 Dryer without Mast, Load Cases 2-14, Maximum Weld Stresses (cont.)

a,c

Table 4–12 PB2 Dryer without Mast, Load Cases 2-14, Maximum Weld Stresses (cont.)

a,c

Table 4–12 PB2 Dryer without Mast, Load Cases 2-14, Maximum Weld Stresses (cont.)

a,c

Table 4–12 PB2 Dryer without Mast, Load Cases 2-14, Maximum Weld Stresses (cont.)

a,c

Table 4-13 PB2 Dryer without Mast, Load Combinations, Maximum Weld Stresses

a,c

Table 4–13 PB2 Dryer without Mast, Load Combinations, Maximum Weld Stresses (cont.)

a,c

Table 4–13 PB2 Dryer without Mast, Load Combinations, Maximum Weld Stresses (cont.)

a,c

Table 4–13 PB2 Dryer without Mast, Load Combinations, Maximum Weld Stresses (cont.)

a,c

Table 4–13 PB2 Dryer without Mast, Load Combinations, Maximum Weld Stresses (cont.)

a,c

Table 4-13 PB2 Dryer without Mast, Load Combinations, Maximum Weld Stresses (cont.)

a,c

Table 4-14 PB3 Dryer, Load Cases 2-14, Maximum Weld Stresses

a,c

Table 4–14 PB3 Dryer, Load Cases 2-14, Maximum Weld Stresses (cont.)

a,c

Table 4–14 PB3 Dryer, Load Cases 2-14, Maximum Weld Stresses (cont.)

a,c

Table 4–14 PB3 Dryer, Load Cases 2-14, Maximum Weld Stresses (cont.)

a,c

Table 4–14 PB3 Dryer, Load Cases 2-14, Maximum Weld Stresses (cont.)

a,c

Table 4–14 PB3 Dryer, Load Cases 2-14, Maximum Weld Stresses (cont.)

a,c

Table 4-15 PB3 Dryer, Load Combinations, Maximum Weld Stresses

a,c

Table 4–15 PB3 Dryer, Load Combinations, Maximum Weld Stresses (cont.)

a,c

Table 4–15 PB3 Dryer, Load Combinations, Maximum Weld Stresses (cont.)

a,c

Table 4–15 PB3 Dryer, Load Combinations, Maximum Weld Stresses (cont.)

a,c

Table 4–15 PB3 Dryer, Load Combinations, Maximum Weld Stresses (cont.)

a,c

Table 4–15 PB3 Dryer, Load Combinations, Maximum Weld Stresses (cont.)

a,c

Table 4-16 All Dryers, Service Levels, Maximum Weld Stresses

a,c

Table 4–16 All Dryers, Service Levels, Maximum Weld Stresses (cont.)

a,c

Table 4-17 Maximum Weld Stresses After Removing Elements at Maximum Stress Locations

a,c

Table 4-17 Maximum Weld Stresses After Removing Elements at Maximum Stress Locations (cont.)

a,c

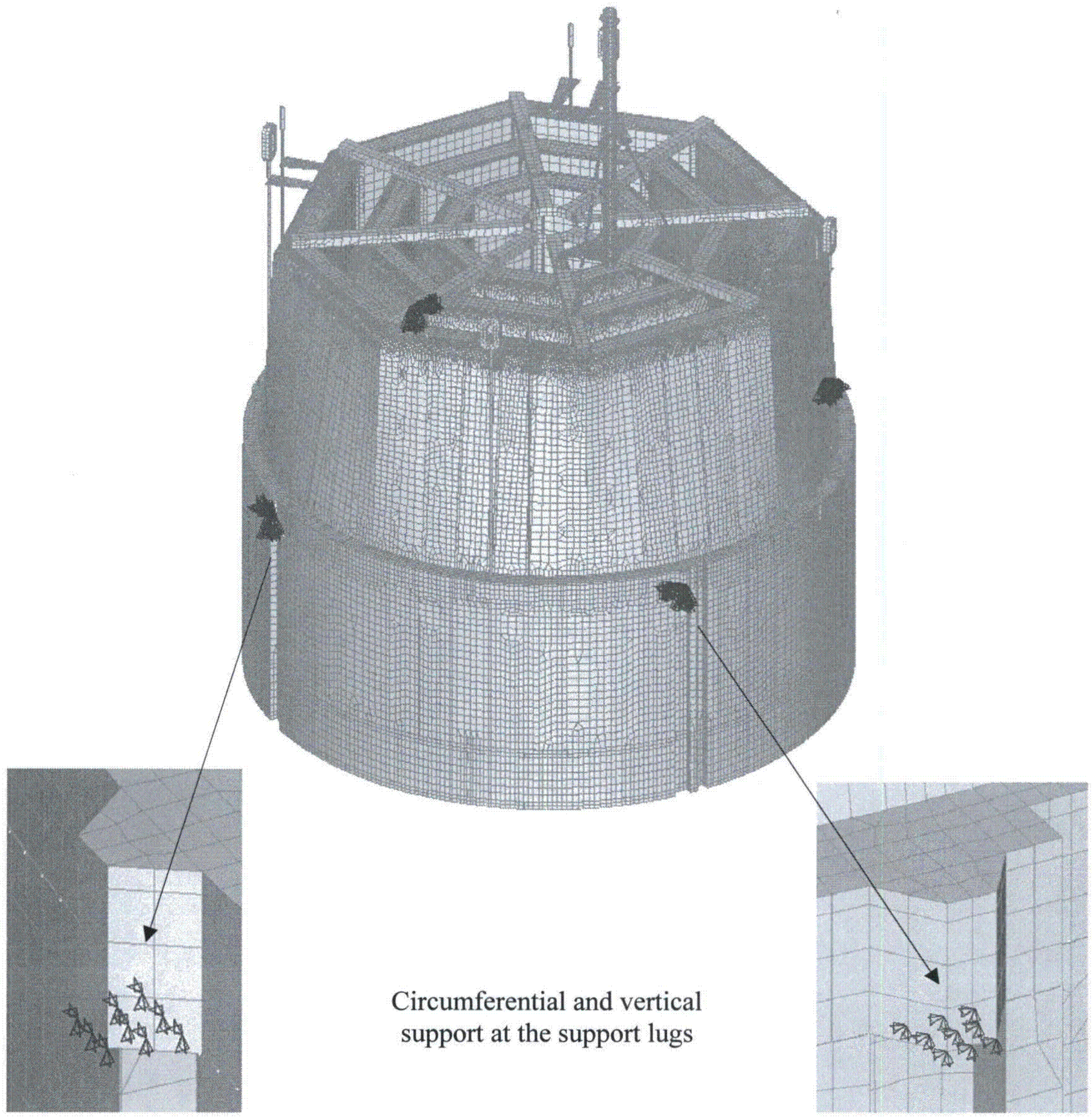

Figure 4-1 Boundary Conditions for Analyses with No Dryer Lift-Off

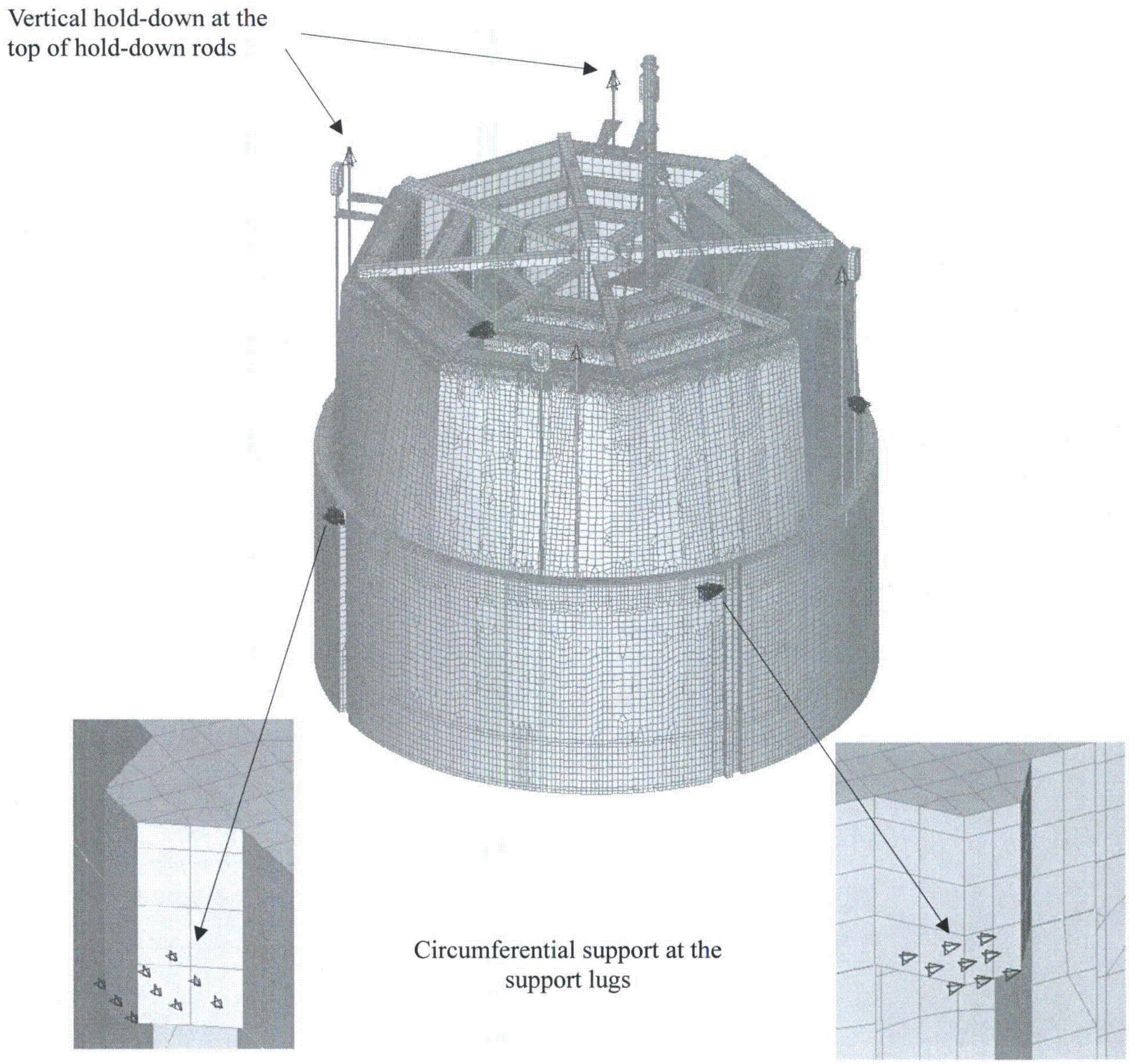

Figure 4-2 Boundary Conditions for Dryer Lift-Off Analysis

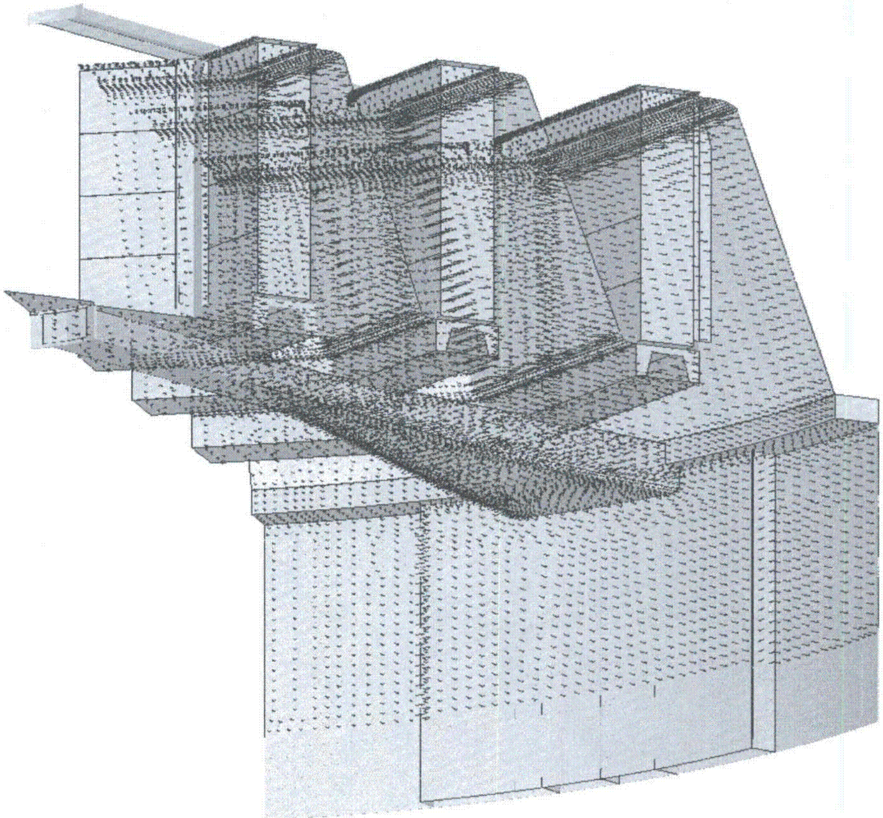

Figure 4-3 Differential Pressure Loads - DP_N, DP_U, DP_E, $MSLB_{DP1}$ and $MSLB_{DP2}$

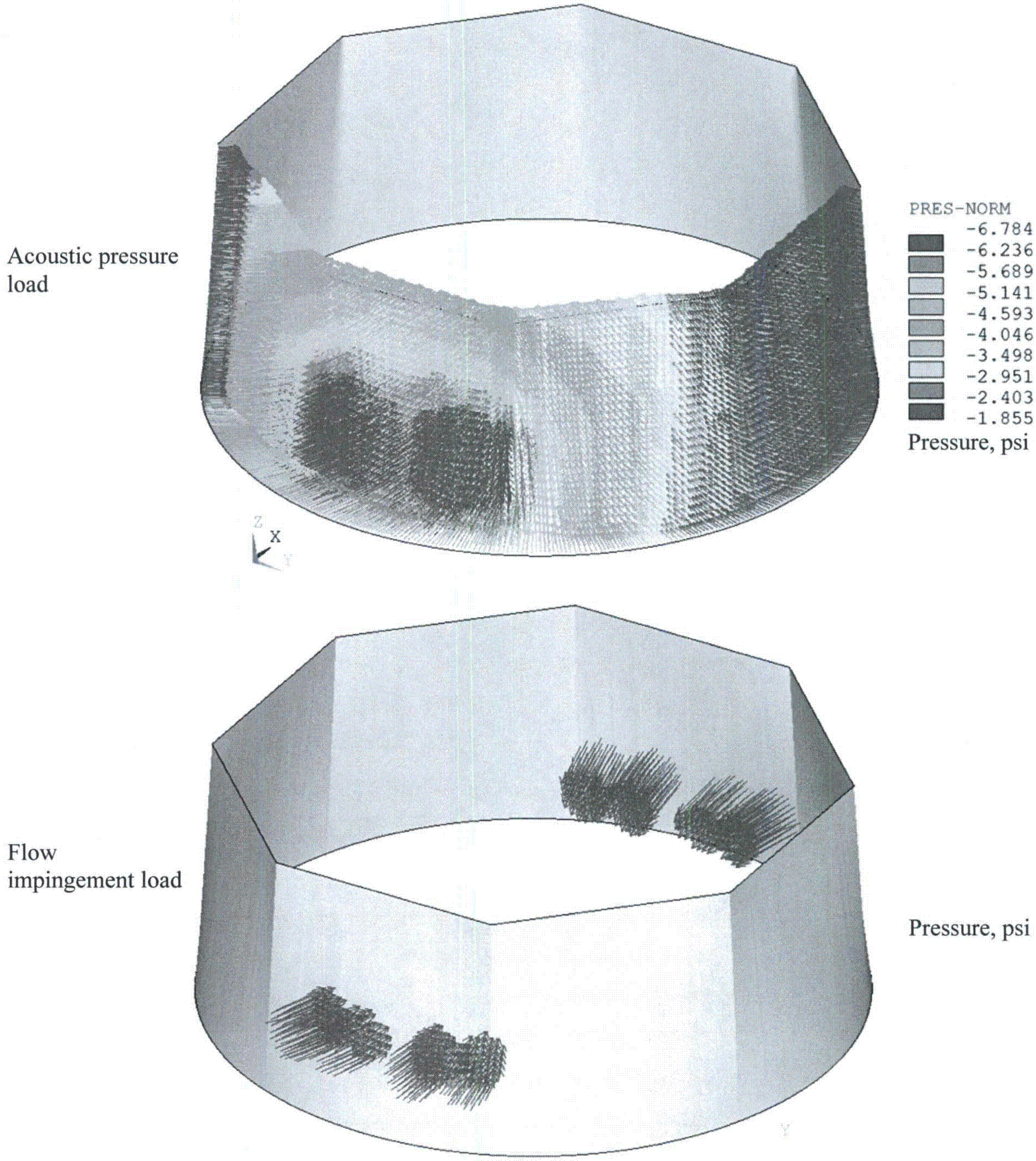

Figure 4-4 TSV Loads - TSV_A, TSV_F

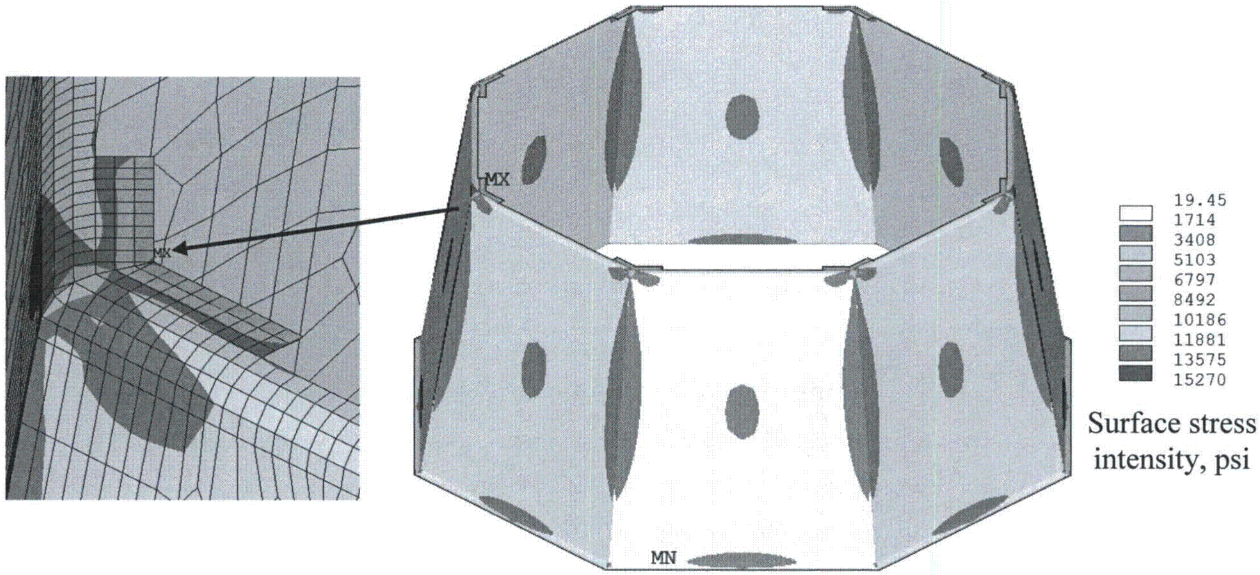

Stress distribution - all elements

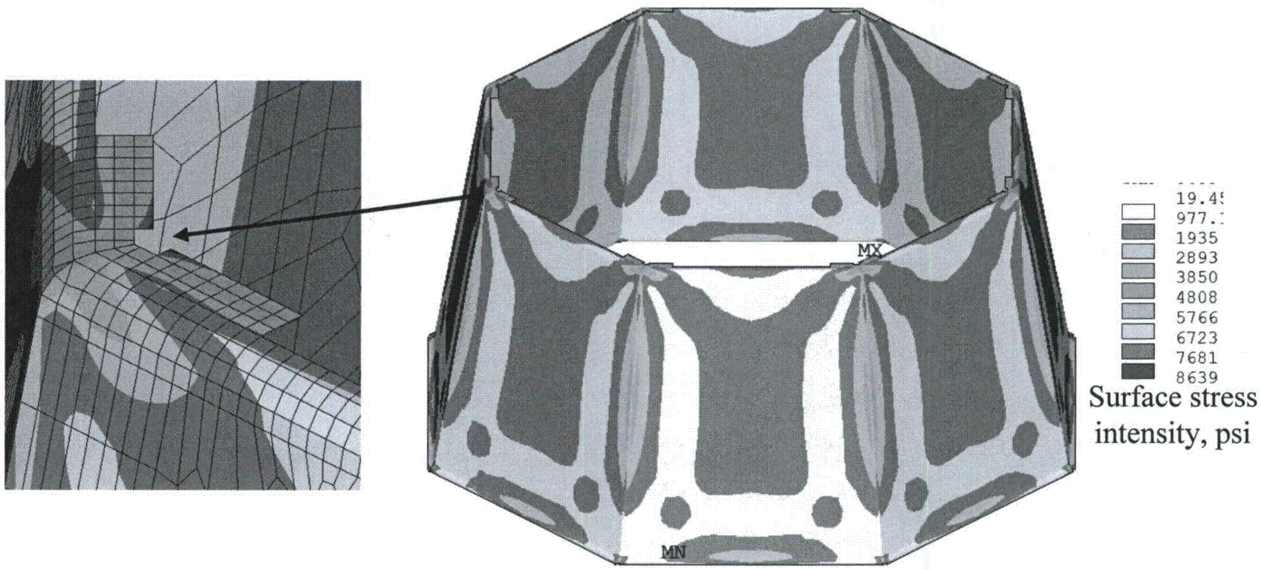

Stress distribution - after removing highest stress elements at multi-plate junctions

Figure 4-5 Surface Stress, Middle Hood: DW + DP_N

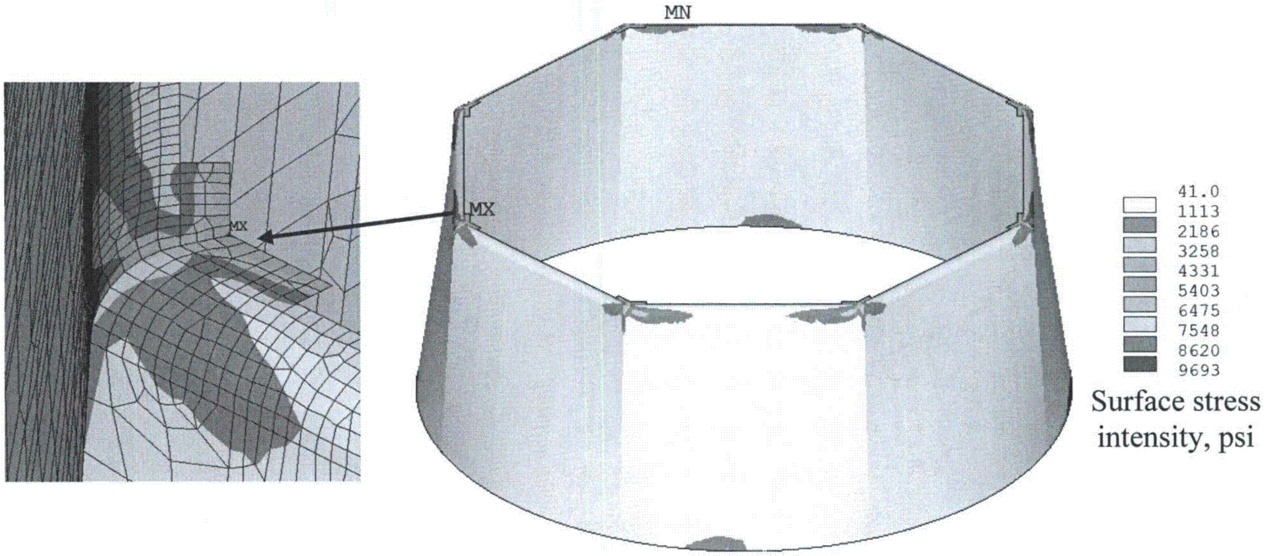

Stress distribution - all elements

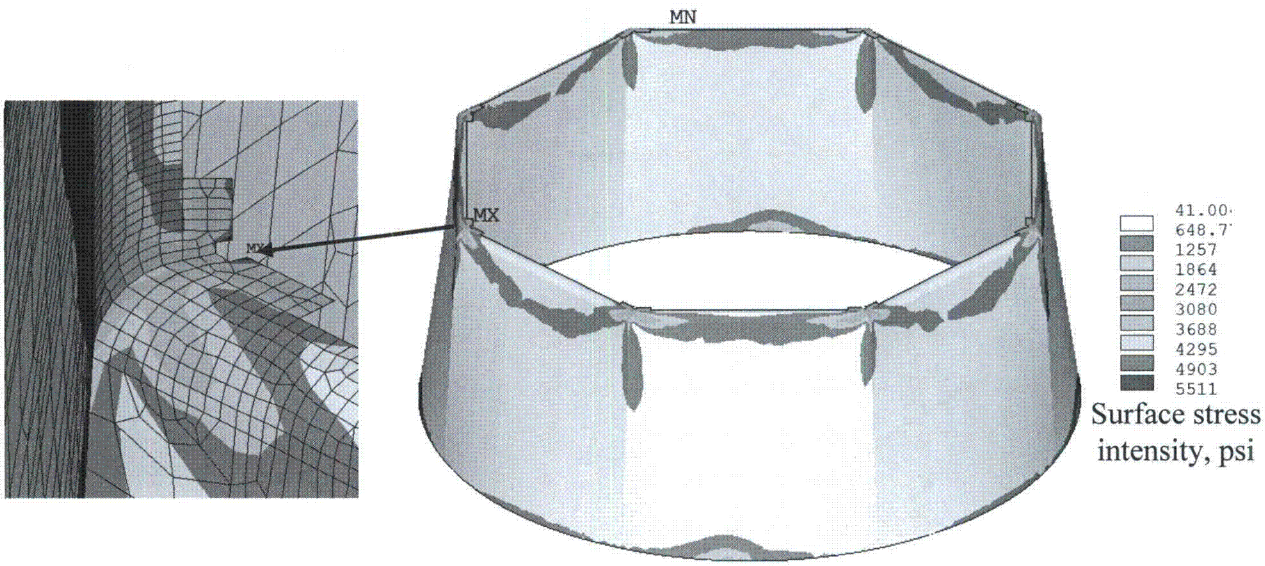

Stress distribution - after removing highest stress elements at multi-plate junctions

Figure 4-6 Surface Stress, Outer Hood: DW + DP_N

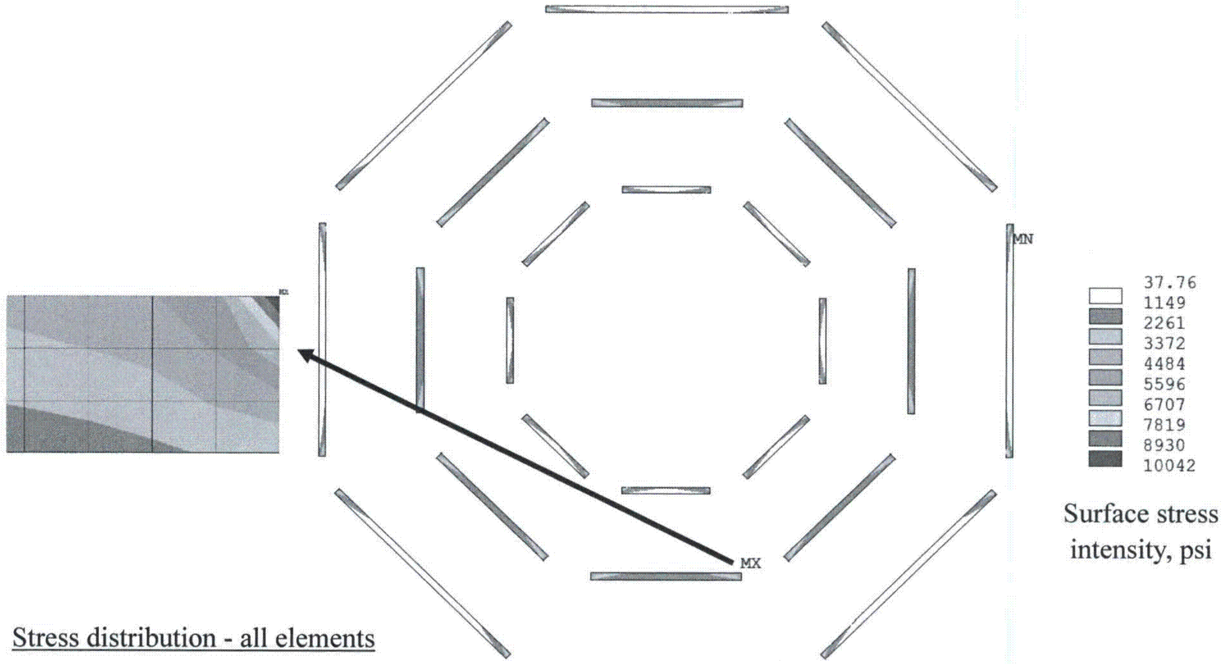

Stress distribution - all elements

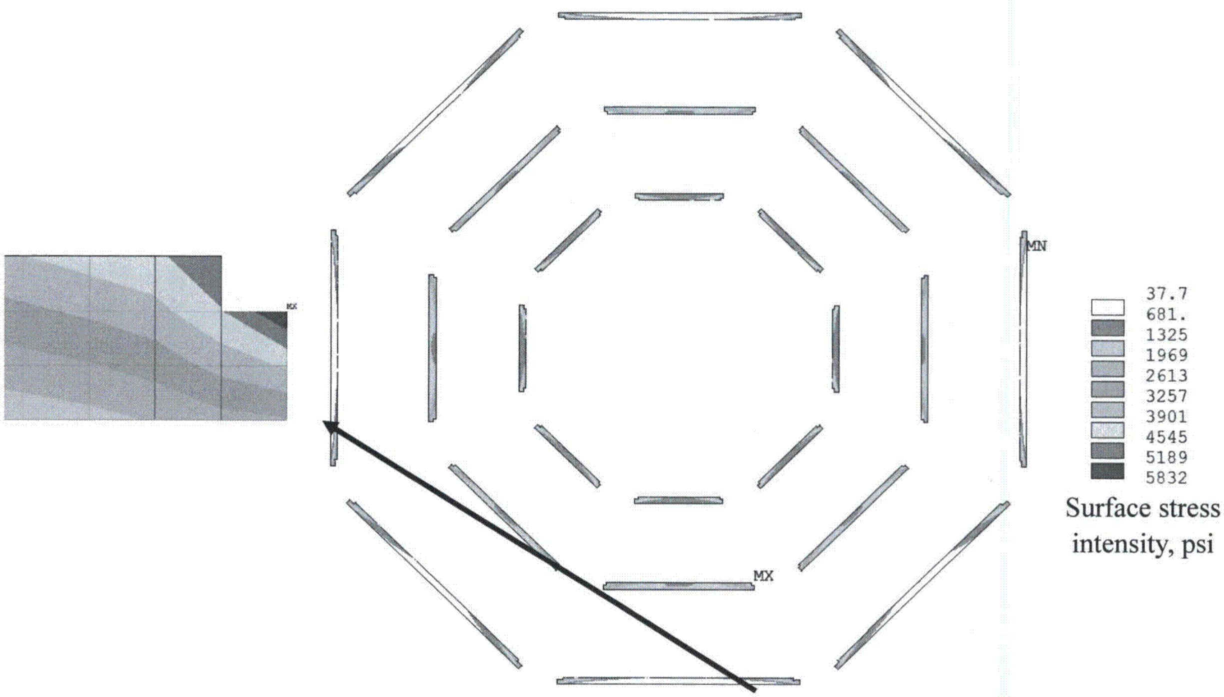

Stress distribution - after removing highest stress elements at multi-plate junctions

Figure 4-7 Surface Stress, Vane Bank Top Steps: DW + DP$_N$

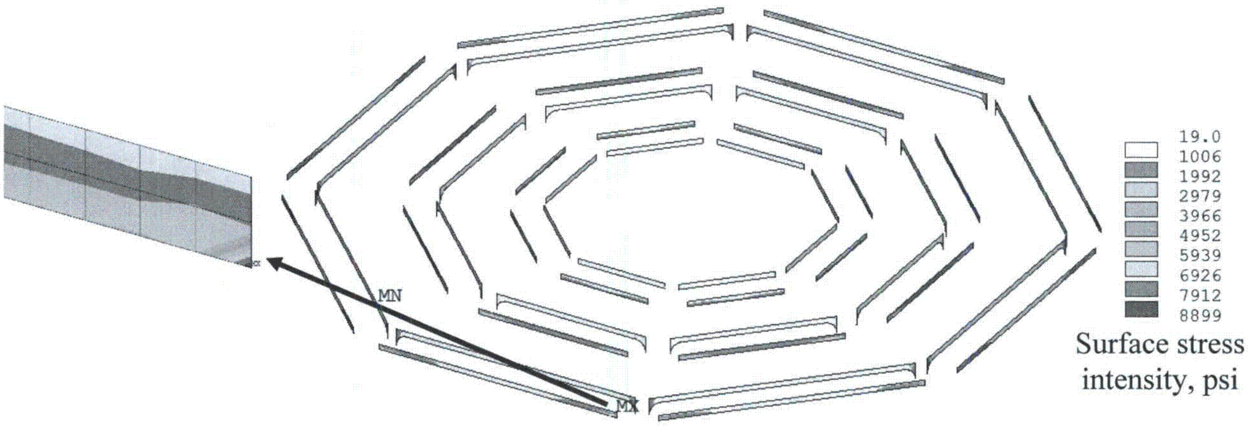

Stress distribution - all elements

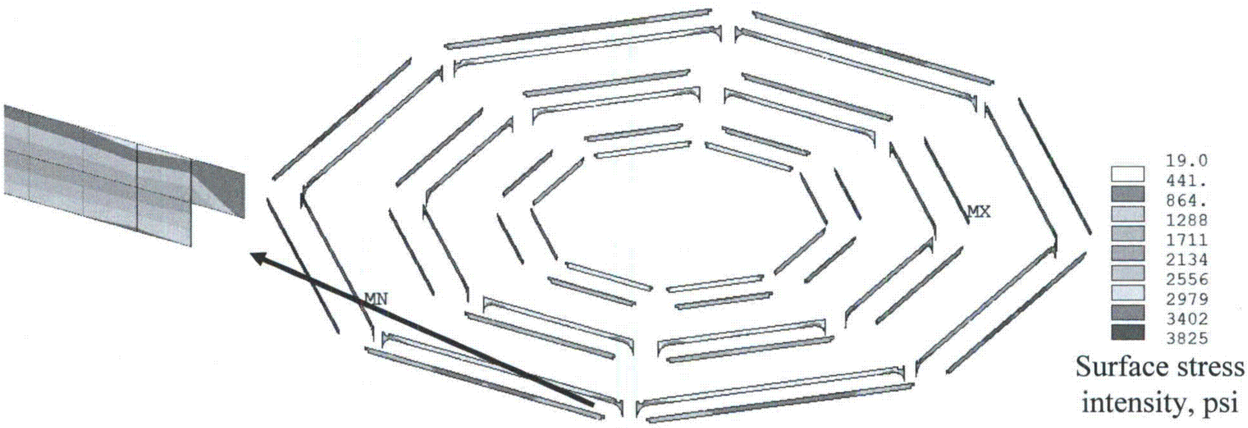

Stress distribution - after removing highest stress elements at multi-plate junctions

Figure 4-8 Surface Stresses, Vane Bank Top Side Plates: DW + DP_N

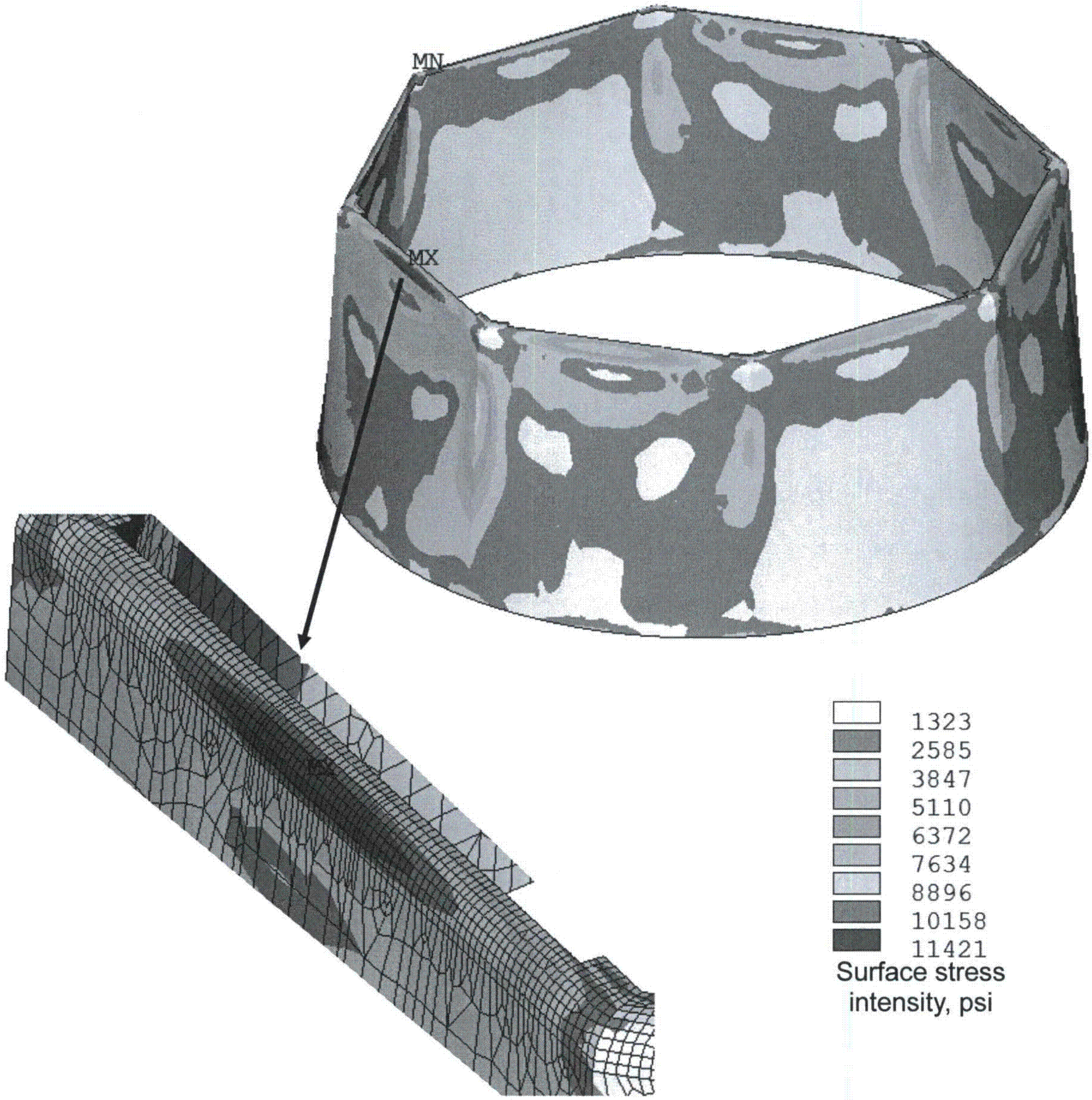

Figure 4-9 Surface Stresses, Outer Hoods: DW + TSV-a

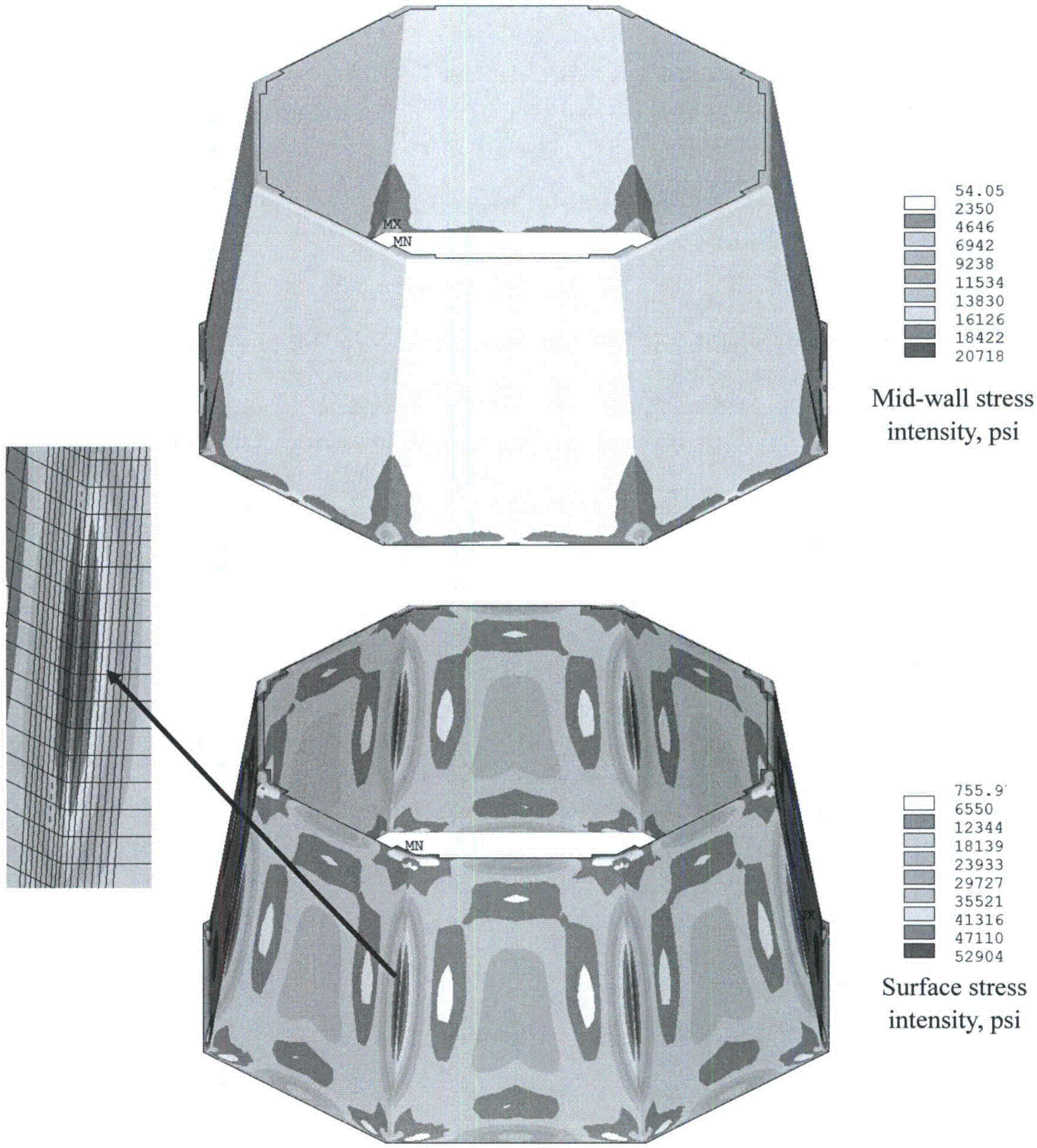

Figure 4-10 Middle Hood Stresses, $MSLB_{DP2}$ Pressure Load

5 DESIGN MARGINS

5.1 STRESS LIMITS

Component design margins are calculated in Table 2-1, Table 2-3, Table 2-5, and Table 2-7 for Service Levels A, B, C, and D, respectively. Weld design margins are calculated in Table 2-2, Table 2-4, Table 2-6, and Table 2-8 for Service Levels A, B, C, and D, respectively.

The dryer components and welds for all the dryer configurations meet the ASME Code stress limits.

5.2 FATIGUE USAGE

A fatigue strength reduction factor of [ ]^{a,c} is conservatively used for all the full-penetration welds as opposed to a fatigue strength reduction factor of [ ]^{a,c} applicable to the component regions away from the welds. Therefore, the largest calculated fatigue usage will be at the welds. The maximum Service Level A and B weld stress of [ ]^{a,c} psi (Table 4-16) is calculated considering all the load combinations including the weight, pressure, FIV/VPF, and OBE stresses. Using a fatigue strength reduction factor of [ ]^{a,c} and ignoring that the weight stresses do not cycle, the cyclic stress range will be [ ]^{a,c} psi, and the stress amplitude will be [ ]^{a,c} psi, from Table 4-16.

For fatigue usage calculations, the stress amplitude is multiplied by the modulus ratio ($E_{ROOM\ TEMPERATURE}$ / $E_{OPERATION}$) = ([ ]^{a,c}, which gives a stress amplitude of [ ]^{a,c} psi. ASME Code permits [ ]^{a,c} cycles operation at this stress amplitude. Assuming the stress cycle applies to all the cyclic loads, the fatigue usage will be [ ]^{a,c} start-up-shutdown cycles + [ ]^{a,c} OBE cycles / [ ]^{a,c}, which is insignificant. FIV and VPF stresses in absence of cyclic pressure and seismic loads are well below the ASME Code endurance limit. Therefore, additional fatigue usage from these loads is negligible.

6 REFERENCES

1. U. S. Nuclear Regulatory Commission, Regulatory Guide 1.20, Rev. 3, Comprehensive Vibration Assessment Program for Reactor Internals during Preoperational and Initial Startup Testing, March 2007.
2. American Society of Mechanical Engineers (ASME) Boiler and Pressure Vessel Code, Section III, Division 1 - Subsection NG, Core Support Structures, 2007 Edition with 2008 Addenda.
3. ANSYS Release 11.0, ANSYS, Incorporated.
4. Westinghouse Document CN-A&SA-12-09, Rev. 2, "Peach Bottom Units 2 & 3 Replacement Steam Dryer Acoustic Structural Analysis."
5. Westinghouse Document CN-A&SA-12-23, Rev. 2, "Main Steam Line Break Acoustic Transient Load Definition for Peach Bottom Units 2 and 3."
6. Westinghouse Document CN-BWR-ENG-12-009, Rev. 0, "Pressure Drop across Exelon Steam Dryers."
7. Exelon Document TODI EPU-DIR-T0305A08, "Reactor Thermal Cycles."
8. Westinghouse Document CN-BWR-ENG-12-002, Rev. 1, "Valve Closure Loads on the Steam Dryer."
9. Westinghouse Document 425A69, Rev. 4, "Design Specification, Exelon Replacement Steam Dryers for PBAPS 2&3."
10. Exelon Document TODI EPU-MOD-RSD-11-0, "Design Parameters for Replacement Steam Dryer Design."
11. American Society of Mechanical Engineers (ASME) Boiler and Pressure Vessel Code, Section II, 2007 Edition with 2008 Addenda.
12. SES 12-207, Rev. 0, "Exelon Replacement Steam Dryer - Limit Analysis of the Middle Hoods for Peach Bottom 2 RSD."
13. American Society of Mechanical Engineers (ASME) Boiler and Pressure Vessel Code, Section III, Division 1 - Appendix F, 2007 Edition with 2008 Addenda.